ISTITUTO NAZIONALE DI FISICA NUCLEARE - ISTITUTO NAZIONALE DI FISICA NUCLEARE - ISTITUTO NAZIONALE DI FISICA NUCLEARE - ISTITUTO NAZIONALE DI FISICA NUCLEARE - ISTITUTO NAZIONALE DI FISICA NUCLEARE - ISTITUTO NAZIONALE DI

Laboratori Nazionali di Frascati

LNF- 90/058(R)
16 Luglio 1990

C. Biscari, S. Kulinski, B. Spataro, F. Tazzioli, M. Vescovi:

MEASUREMENTS ON THE NEW INJECTION SYSTEM OF THE FRASCATI LINAC

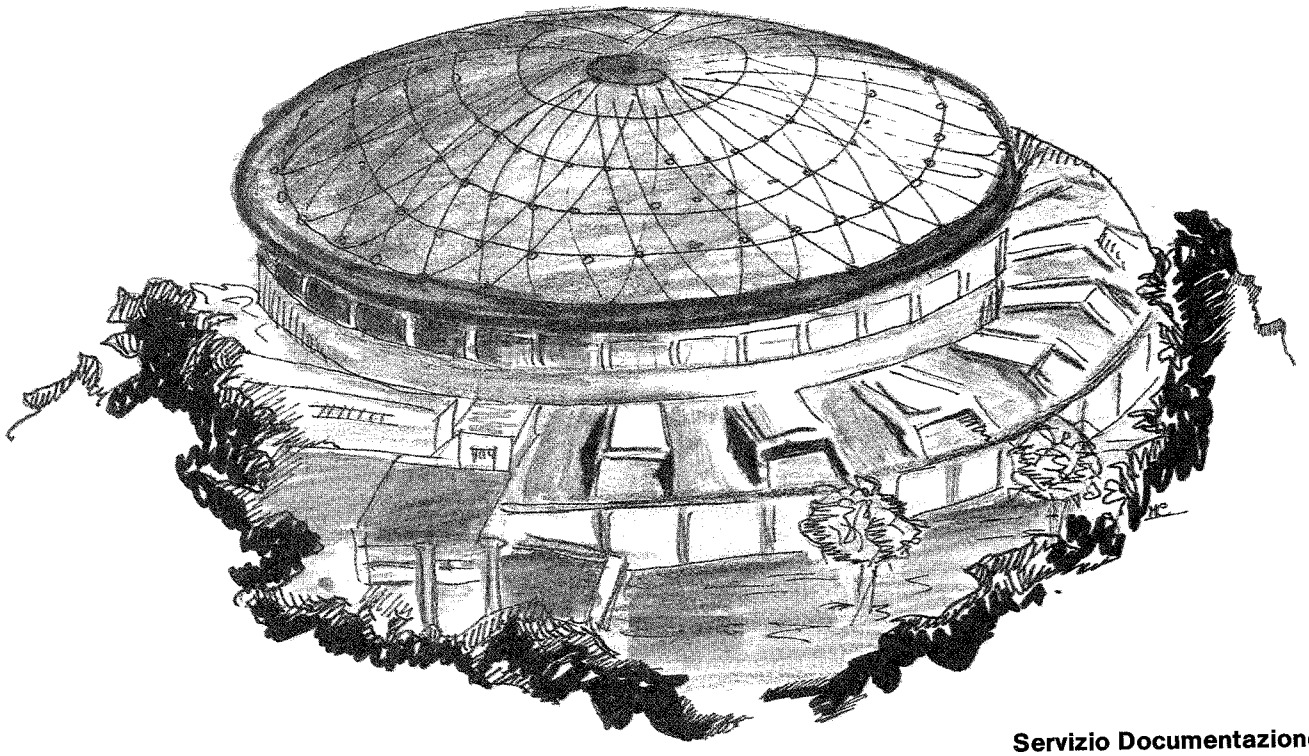

Servizio Documentazione
dei Laboratori Nazionali di Frascati
P.O. Box, 13 - 00044 Frascati (Italy)

INFN - Laboratori Nazionali di Frascati
Servizio Documentazione

LNF-90/058(R)
16 Luglio 1990

MEASUREMENTS ON THE NEW INJECTION SYSTEM OF THE FRASCATI LINAC

C. Biscari, S. Kulinski, B. Spataro, F. Tazzioli, M. Vescovi
INFN, Laboratori Nazionali di Frascati, P.O.Box 13, 00044 Frascati (Italy)

1. - INTRODUCTION

Recently at Frascati LNF a new injection system for the 400 MeV e+ e- linac [1] has been installed. The new elements in this system are: the gun and the standing wave buncher [2]. The aim of this operation was to increase the rate of positron production and to shorten in this way the accumulation time of positrons in the ADONE ring. The new gun delivers a higher peak current (up to ≈ 15 A) with a shorter pulse duration (≈ 10 ns)with respect to the old Mark IV Varian gun.

During installation a set of measurements has been made concerning the performance of the new injector of the linac and its adaptation to other components of ADONE positron and electron injection system. Especially the transmission efficiency along the linac and energy spread at its end have been measured. The results of these measurements have inspired some modification in the originally proposed system e.g. by adding a separate prebuncher to increase the efficiency of positron production and transport to the ring.

The present paper describes possibly chronologically the performed measurements and discusses the obtained results.

2. - LAYOUT OF THE INJECTION SYSTEM

The layout of the linac and the used measuring instrumentation is shown in Fig. 1.

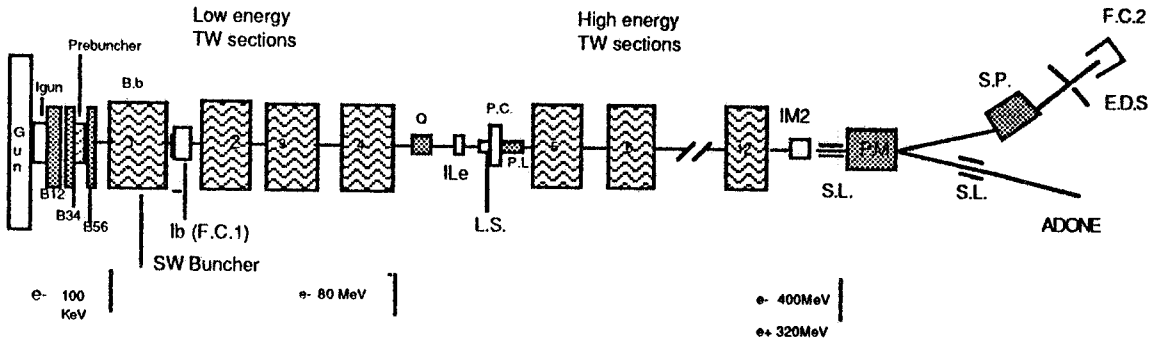

Igun capacitive electrode
Ib capacitive electrode
ILe wall current monitor
IM2 wall current monitor
F.C.1, F.C.2 FARADAY cup
B12 gun solenoids
B34 double thin lenses
B56 double thin lenses
Bb buncher solenoid
Q quadrupole triplet

P.C. positron converter
P.L. positron lens
S.L. strip line monitor
P.M. pulsed magnet
S P. spectrometer
E.D.S. energy defining slits
L.S. luminescent screen

FIG. 1 - Layout of the ADONE injector LINAC

The main components of the system are:

- Electron gun
- Prebuncher
- Standing wave buncher
- 3 low energy TW accelerating sections ($\Delta E \approx 80$ MeV)
- 8 high energy TW accelerating sections ($\Delta E \approx 320$ MeV , for $I \approx 0$ A)
- Electron positron converter together with focusing system.
- Beam transport and focusing system composed of solenoids and quadrupoles (not shown in Fig. 1.)

The main parts of the linac remained unchanged and its detailed description can be found in the existing literature [1]. The new components are practically the gun and the SW buncher The main parameters of these components are given below.

2.1 - THE GUN

The gun is a triode of the Pierce type made by CGR MEV and is similar to that used in the LIL-LEP injector. The main parameters of this gun are:

- Maximum potential difference cathode-anode $V_{ak} = 100$ kV.
  Dark current $I_m < 1\mu a$.
  Maximum repetition frequency $F_r = 200$Hz.

Current parameters:

a) long pulses

40 ns -2 μs $I_{max} = 3$ A
rise time from 20% to 80% of I_{max} t = 10ns.
2 μs - 4 μs $I_{max} = .77$ A. For 4 μs $I_{ont} = 120$ mA.

b) short pulses
t_{min}= 3 ns , I_{max} = 6 A
t_{max}= 20 ns , I_{max} = 15 A
rise time (20- 80)% of I_{max} t = 1.3 ns.
time of descent (80-20)% of I_{max} t ≈ 2 ns.

2.2 - STANDING WAVE BUNCHER

The buncher was designed and constructed by CGR MeV together with the gun specially for the ADONE injector. Taking into account the good results obtained with high field mode operation experimented in LIL - LEP prebuncher, in which the bunching process was practically accomplished inside the cavity of the prebuncher [3,4,5] , it was decided not to use a separate prebuncher but incorporate it in one cavity with the SW buncher. The optimization of the bunching and phase acceptance of the system is made by adjusting the ratio $R = E_1/E_2$, where E_1 nad E_2 are the electric field intensities in the first and in the second cells of the accelerating section correspondingly. The buncher is a standing wave $\pi/2$ biperiodic section with the only exception of the first capture cell which has a π phase shift. The main parameters of this section are:

the length of the section	L = 1.16 m
Number of cells of the $\pi/2$ type	N = 23
Capture cell (π mode)	N =1
Diameter of iris	D = 27 mm
Entrance and exit diameter	D_i = 16 mm
Frequency	F_r = 2856 MHz
Power input	P = 10 MW
Energy increase	ΔW = 20 MeV (I ≈ 0)
Solenoidal magnetic field	B = 1200 - 1500 Gs

According to the CGR MeV calculation [5] the optimum value of R is close to R = 0.5. In this case the phase acceptance is at least 56% and the bunch length at the exit of the buncher is 45°-50°. We will come back to this point when discussing the results of measurements. E.g it will be shown that for positron production with sufficiently small energy dispersion necessary for the injection into the ring it is important to have at the e^-e^+ converter a short ($\Delta\Phi \approx 15°$) well collimated electron beam.

2.3 INSTRUMENTATION USED FOR MEASUREMENTS

The distribution of monitors and other instruments used for measurements is shown in Fig. 1. Below we give some additional informations on this instrumentation:

I_G - Electrostatic electrode placed behind the anode of the gun to measure the current of the gun. For pulse length $t_p \approx 10$ ns the sensitivity is 0.066V/A.
I_B - Electrostatic electrode placed behind the SW buncher. Sensitivity (for $t_p \approx 10$ ns) 0.6V/A. Remark - the signal from this electrode was rather unusual having two peaks: positive and negative The calibration is for the higher negative peak.
I_{LE} Wall current monitor to measure the current of low energy electrons (before the e^-e^+ converter). Sensitivity for $t_p \approx 10$ ns -0.350V/A.
I_{M2} Wall current monitor to measure the current at the end of the linac. Sensitivity - 0.8 V/A.
FC1,FC2 - Faraday cups.

L.S. - Luminescent screen to observe the beam position and dimensions.
P.M. - Pulsed magnet , deflecting angle 6° at 300 MeV.
SP. - Magnetic spectrometer , deflecting angle 60°.
S.L. - Strip line monitors.

The beam position and dimensions can be observed on the luminescent screen which could be inserted at the position of the positron converter. Similar screen was also used when measuring at the exit of the buncher. At the end of the high energy linac the strip lines were used to detect the value and the position of the beam.

3. - MEASUREMENTS WITHOUT PREBUNCHER.

The first measurements with the new injection system were made without the prebuncher. The SW Buncher was connected directly to the gun. The results of these measurements are given in Table I. They have evidenced two pricipal features:

1. A low transmission efficiency of the system. About 30% of transmission up to the positron converter and only from 15% to 30% transmission in the high energy part of the linac the lower transmission corresponding to higher currents. As a result the overall transmission efficiency was about 10% or lower.
2. A large energy spread between 10 and 35 MeV (= 2-10%) for gun currents between 1 A and 10 A.

TABLE I - Measurements of the electron beam characteristics in the new injection system.

I_{gun} (A)	I_{LE} (A)	I_{M2} (A)	η_1	η_2	η	E_{EDS} (MeV)	$\langle I \rangle_{FC}$ (nA)	t (ns)	I_{pFC} (mA)	ΔE_{EDS} (MeV)	η_3
0.67	0.21	0.07	0.32	0.32	0.10	340.	0.10	6.5	15.0	-	0.22
1.00	0.30	0.11	0.30	0.37	0.11	340.	0.14	6.2	22.5	7.	020
1.06	0.31	0.09	0.30	0.30	0.09	330.	0.15	6.0	25.0	-	0.27
2.27*	0.73	0.21	0.32	0.28	0.09	340.	0.20	7.5	27.0	15.	0.13
3.03	1.00	0.23	0.33	0.23	0.07	335.	0.40	7.2	55.0	10	0.24
2.27**	0.61	0.24	0.27	0.38	0.10	330.	0.20	7.5	26.0	10.	0.11
5.30	1.62	0.39	0.31	0.24	0.07	325	0.38	7.5	50.6	30.	0.13
7.57	2.45	0.44	0.32	0.18	0.06	320	0.42	8.0	50.0	30.	0.11
9.09	3.08	0.55	0.34	0.18	0.06	320	0.38	7.5	50.6	15.	0.09
9.09**	3.14	0.09	0.35	0.12	0.01	325	0.25	8.5	30.0	35.	0.04
11.36	3.78	0.54	0.33	0.14	0.05	320	0.38	8.0	47.5	35.	0.09

Inversion of the magnetic field direction in the SW Buncher (the magnetic field has the same direction all along the low energy part of the Linac)

3.18	0.90	0.40	0.29	0.44	0.12
2.00	0.57	0.23	0.29	0.40	0.11

*Measurements of the energy gain by switching off the modulators

Modulator	1	2	3	4	5	
E_{tot} (MeV)		283.	255	255.	257.	342.

Number of switched off modulator		2	3	4	5
Energy gain (MeV)	24.	59.	87.	87.	85.

** The current in the solenoids in the high energy part is equal to 200A. The other measurements were done with zero magnetic field.

$\eta_1 = I_{LE}/I_{gun}$, $\eta_2 = I_{M2}/I_{LE}$, $\eta = I_{M2}/I_{gun}$, $\eta_3 = I_{pFC}/I_M$

A discussion of these results is given in [6] here we will give some specific points. The efficiency of beam transmission through the whole linac depends on many parameters such as: beam emittance, phase acceptance of the linac, especially of the low energy part where the beam is not yet relativistic and large phase oscillations exist, alignment of the accelerating sections and focusing elements of the transport system.

We found particularly puzzling the large losses in the high energy part of the linac where the particles are already relativistic, and the phase oscillations ,as well as the space charge forces , should be already small and usually the beam should propagate without excessive losses. A possible explanation of obtained results could be that the beam emittance is very large so that the existing focusing system was not adequate to transmit the beam properly or that there existed large misalignements in the transport and focusing systems. Below we will see that the main cause of these losses is the large beam emittance.

To have some idea on the beam parameters at the beginning of the accelerating system additional measurements have been made at the end of the SW buncher. They consisted of:

- Beam position and dimension measurements
- Current distribution across the beam.
- Transmission efficiency
- Energy measurements

To make these measurements possible an additional Faraday cup has been installed at the exit of the SW buncher together with a removable luminescent screen for beam position and dimension measurements (see Fig. 2). The results are described below.

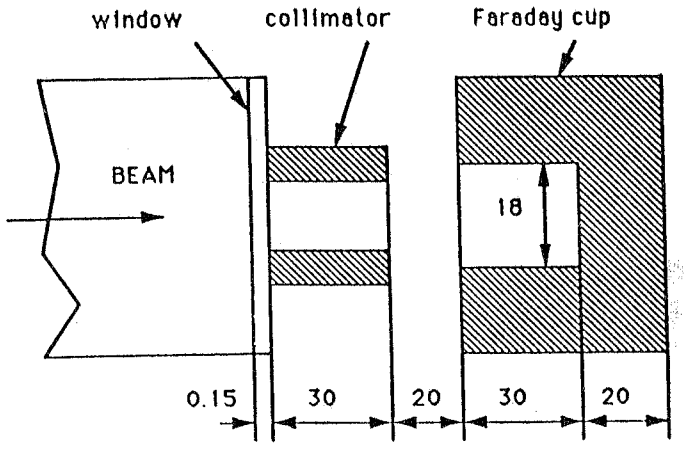

FIG. 2 - Measuring Set at the End of the SW Buncher. All dimensions are given in mm.

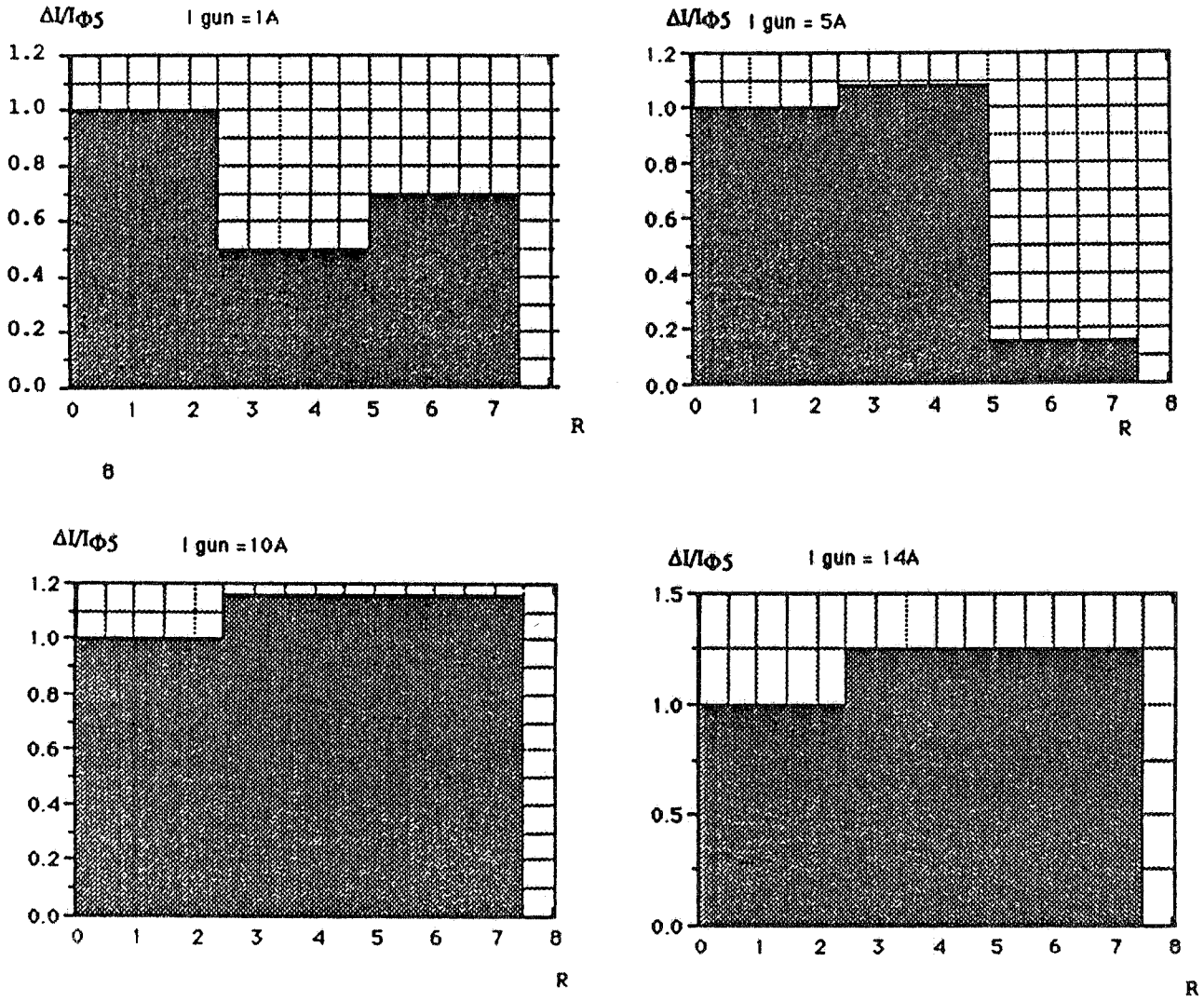

FIG. 3 - Relative Current Distribution $\Delta I/I\Phi 5$ along the beam radius. ΔI-current contained in the ring with $\Delta R = 2.5$ mm, $I\Phi 5$-current contained in the cylinder of the diameter $\Phi = 5.0$ mm in the vicinity of the axis

3.1 - BEAM POSITION AND DIMENSION MEASUREMENTS AT THE EXIT OF THE SW BUNCHER

The beam was observed at a ceramic luminescent target behind a 0.15 mm stainless steel window which closed the buncher. The dimension and the position of the beam depended on the gun current and on the values of the currents in the focusing solenoids connected with the gun and the buncher. The diameter of the beam changes roughly from 10mm to 20mm when the gun current changes from 3 to 15 A. Without steerings the beam center position depends on the gun current Ig. For Ig = 3 A it is displaced vertically about 5mm upwards and for Ig = 10A about 2-3mm to the right. With the aid of two pairs of steering it was always possible to put the center of the beam on the geometrical axis of the channel. However the angle between the beam and the geometrical axis of the system remains unknown. The results of these measurements are presented in Figs. 3, 4 and will be discussed below.

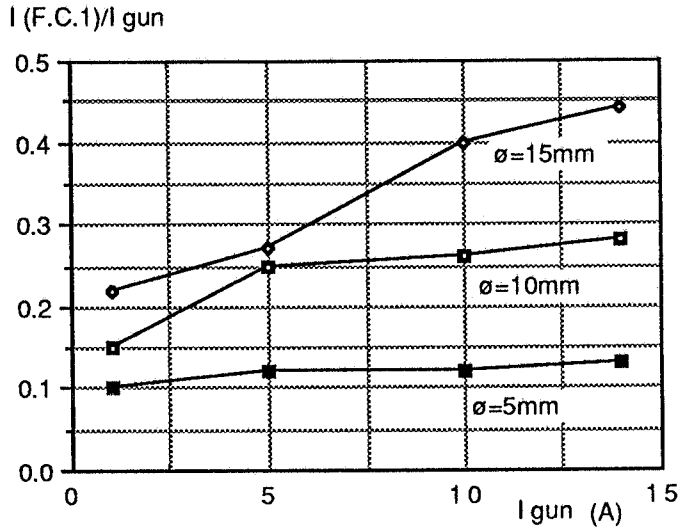

FIG. 4 - Transmission efficiency I_Φ/I_{gun} as a function of the gun current I_{gun} and the collimator diameter Φ.

3.2 - TRANSMISSION EFFICIENCY AND CURRENT DISTRIBUTION AT THE EXIT END OF THE BUNCHER

The first surprising result of these measurements was the very large beam diameter with probable large divergence. For Ig ≥ 10 A the beam occupies the whole cross-section of the exit hole of the buncher having diameter of 16mm and in few milimeters diverges to about 20 mm. To measure the radial current distribution we have used four collimators with the diameters Φ = 5, 10, 15, and 30 mm followed by the Faraday cup. The measuring set is shown on Fig. 2 and the results are given in Table II and also presented in Figs. 3, 4. They can be summarized as follows:

- In agreement with the images on the luminescent screen the beam occupies practically the whole cross-section of the exit flange having diameter Φ = 16mm. For Ig ≥ 10 A the current ΔI contained in the rings of width ΔR = 5mm is practically constant.
- For small collimator diameter Φ = 5mm the transmission efficiency is practically independent o f the gun current . It means that the radial current distribution in the vicinity of the axis does not depend on Ig.For large collimator diameters the transmission efficiency increases monotonically with the gun current and is about two times larger for Ig = 14 A in comparison with Ig = 1 A. Taking into account that the current distribution in the vicinity of the axis practically does not depend on Ig it means that the charge distribution in the beam increases along the radius (at least in some region) with increasing Ig. This tendency is also seen on the distribution of the current ΔI along the radius.

Using these informations we can try to explain some results given in Table I concerning the low tranmission efficiency of the measured injection system. It is obvious that a beam with such a large diameter and probably with very large emittance cannot be transported without losses through the following TW sections . What we can expect is the transmission of the beam with the diameter not very much larger than about Φ = 5mm and for this beam the efficiency at the buncher exit is a little higher than 10% which agrees well with the overall efficiency at the end of the linac. The question then arises why the emittance of the beam is so large . It seems that to find the answer we should investigate the performances of the gun and the transport system between the gun and the buncher. Since we have not had the measured results we tried

to calculate some characteristics of the gun using the SLACGUN program of Hermannsfeldt. (see. 3.4)

TABLE II - Measurements of the current transmission along the Linac.

Φ = Diameter of the collimator at the end of the SW Buncher				
Φ = 5mm				
I_{gun} (A)	1.	5.	10.	14.
τ (ns)	6.	7.	7.3	7.5
<I> (nA)	1.8	13.	27.	40.
I_{peak} (A)	0.1	0.62	1.23	1.77
$\eta = I_{peak}/I_{gun}$	0.1	0.12	0.12	0.13
Φ = 10mm				
I_{gun} (A)	1.	5.	10.	14.
τ (ns)	6.3	6.24	7.32	7.7
<I> (nA)	2.9	23.	58.	90.
I_{peak} (A)	0.15	1.23	2.64	3.9
$\eta = I_{peak}/I_{gun}$	0.15	0.25	0.26	0.28
Φ = 15mm				
I_{gun} (A)	1.	5.	10.	14.
τ (ns)	7.6	7.6	7.6	/
<I> (nA)	5.	30.	85.	/
I_{peak} (A)	0.22	1.32	3.75	/
$\eta = I_{peak}/I_{gun}$	0.22	0.26	0.38	/
Φ = 30mm				
I_{gun} (A)	1.	5.	10.	14.
τ (ns)	6.14	7.0	7.6	7.7
<I> (nA)	4.	28.	90.	140.
I_{peak} (A)	0.22	1.33	3.95	6.1
$\eta = I_{peak}/I_{gun}$	0.22	0.27	0.40	0.44

REMARK

There is some disagreement between the results given in Table I and those obtained with the aid of Faraday cup at the end of the buncher. Namely according to Table I the transmission efficiency up to the positron converter is for Ig = 1 A about 0.3, whereas that measured directly at the exit of the buncher is smaller being only 0.22. It seems that this discrepancy can be explained by the use of different measuring devices: wall current monitor in the first case and the Faraday cup in the second. To avoid such problems in further measurements a calibration have been made for all our monitors. The results of these calibrations are given above in chapter 2.3.

3.3 - MEASUREMENTS WITH ADDITIONAL FOCUSING SOLENOID BETWEEN SW AND TW SECTIONS

Taking into account large electron beam dimensions at the exit of the SW buncher it was suggested to introduce a focusing solenoid directly behind the SW section. The parameters of this solenoid are:

Diameter	D = 16 mm
Length	L = 165mm
Maximum field intensity	B_m = 5000 Gs

We have then repeated practically all the measurements presented in Table I. The main results of these measurements are:

- The values for the steering of the SW buncher remained unchanged. It means that the alignement between the beam and the geometrical axis is good
- There is a collimation effect introduced by the solenoid: the transmission up to the positron converter is diminished almost twice being now only about (14-15)% for Ig ≤ 5 A and about 18% for Ig≥ 10A. Without the solenoid the transmission was about 30%. This is the effect of the smaller diameter Φ = 16mm of the solenoid. On the other hand the transmission efficiency of the high energy part is increased to (30-50)% so that the total transmission is almost unchanged and is (5-9)%.
- There is no effect of the magnetic field of the solenoid on the transmission. The results remained practically unchanged with and without the field in the solenoid.

3.4 - SIMULATIONS OF THE GUN PERFORMANCE USING SLACGUN CODE

To have some idea of the beam parameters at the entrance of the buncher we have used the SLACGUN program of Hermannsfeldt to calculate the gun performance. The calculations were made without the axial magnetic field and with the magnetic field for two different cases:

a) Without the prebuncher. In this case the buncher was connected directly to the gun so that the magnetic field was composed of that corresponding to two coils of the gun itself and the quasi uniform magnetic field of the buncher rising up to the value of 1500 Gs.

b) With the prebuncher. In this case two doublets of thin coils one before and one after the prebuncher were added to provide the additional focusing. The values of the field level were calculated using the PARMELA program and are given in Table III. The main results of these calculations are: (See Figs. 5, 6).

- Without the magnetic field the beam is rather strongly focussed inside the anode and then rapidly diverges indicating the necessity of magnetic focussing to confine it inside the transmission tube having the diameter of 16mm.
- There exists rays crossing in the vicinity of the focus what makes the beam flow nonlaminar and can cause some errors in beam characteristics calculations. The crossing of the rays is much stronger in the presence of the magnetic field.
- In the presense of the magnetic field the beam flow is far from having the characteristics of the Brillouin flow: there exist large scallops which can lead to the beam losses and can also cause inhomogeneities in current distribution across the beam, eg. that the the current density increases toward the edge of the beam.

- Usually the beam losses succeeded beyond the position of the first capacitive electrode measuring the gun current. This means that the main beam losses could be in the transmission line before the buncher and can be due to the large amplitude of beam scalloping.
- It is clear that to analyze the beam behaviour it is necessary to proceed the calculation far beyond the anode of the gun.
- The beam emittance changes along the transmission channel and can increase above $5*10^{-4}$ mrad. However it should be taking into account that due to the rays crossing there can be large errors in emittance calculations.

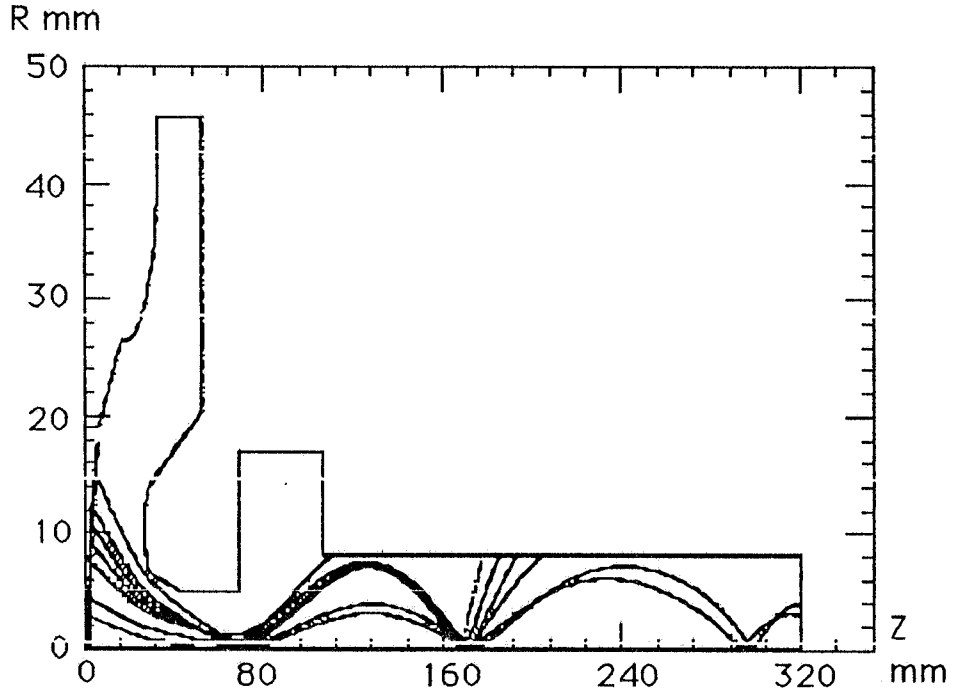

FIG. 5 - ADOONE GUN. Va 90 kV, Vg=940, Ig=27 A. Perveance = 1 microperv, ε_n = 1.9 10^{-3} mrad (nonlaminar flow). Maximum field at the buncher 1500 Gs. No Prebungher.

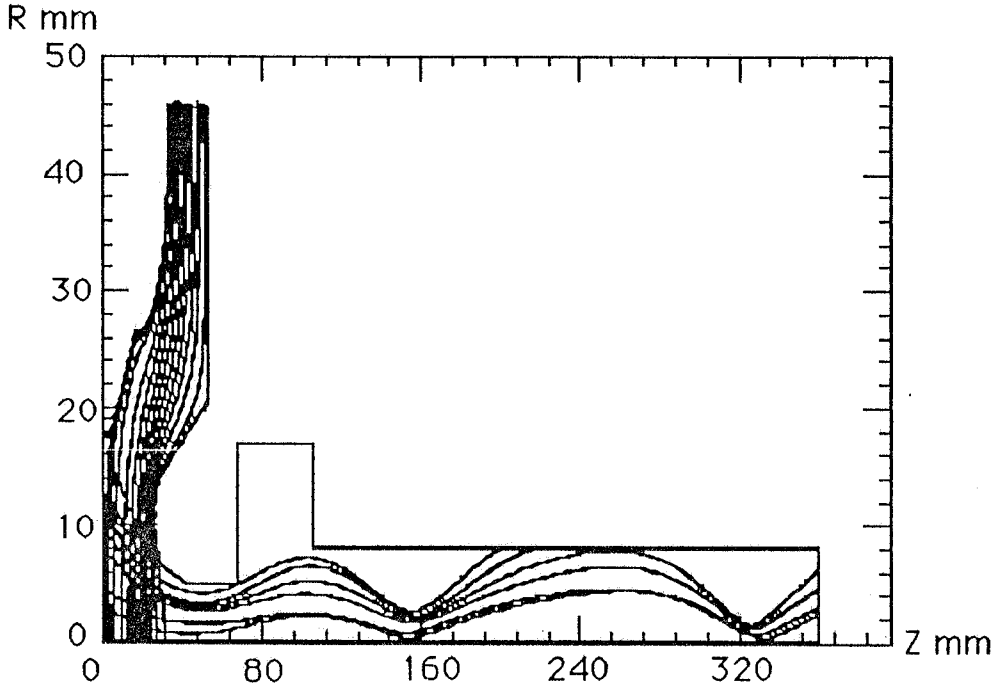

FIG. 6 - ADOONE GUN. Va 90940V, Vg=940, Dkg=1.5 mm, I = 32.3 A, Perveance = 1.18 microperv, ε_n = 4.37 10^{-4} mrad (nonlaminar flow). Maximum field at the buncher 1500 Gs. No Prebungher.

3.5 - ENERGY MEASUREMENTS AT THE EXIT OF THE BUNCHER

For energies in the range up to 20 MeV a simple and sufficiently precise method of measuring the energy of electrons is by finding the thresholds of reactions (γ,n) for different elements. It is known that the neutron binding energies vary through the periodic table from 1.67 MeV for Be^9 to about 19 MeV in carbon C^{12}. The method of measuremet is now the following. Since the energy of electrons accelerated in the linac is roughly proportional to the square root of the input rf power, one starts with some power level lower than that corresponding to the threshold energy of a given element and then increases the power up to the moment when the irradiated matter indicates the existance of the induced radioactivity. Using elements with different thresholds one can find the dependence of the energy of accelerated electrons on the input power. If the beam current is also known it is possible to find the effective shunt impedance of the accelerating structure.

The details of the measurements of the ADONE SW buncher are presented in [7] . Here we will give only the results. Two elements have been activated: carbon C^{12} and iron Fe. It was found that for the input power to the SW buncher of 8 MW and about 6 nC of electrons accelerated in the bunch the output energy was within the limits

$$17.0 \text{ MeV} < W < 19.0 \text{ MeV}$$

The corresponding shunt impedance of the structure was $Z_{sh} \approx (41 - 45)$ MΩ/m.

4.0 - ENERGY AND PHASE DISPERSION. NECESSITY OF A PREBUNCHER

Up to now we have discussed the transmission losses along the linac. We have arrived at the conclusion that the measured poor transmission is mainly due to the large emittance of the beam leaving the gun and scalloping in the transport system between the gun and the buncher. There is however, another problem which must be solved to have both high efficiency of positron creation and and high efficiency of injection of electrons and positrons into the ring. This is the energy spread of both types of particles along the linac and espescially at the positron converter and at the end of the high energy linac. The requirements for good injection are ±1% of energy spread before the injection. However,according to the Table I the energy spread at the end of linac can be about 10-30 MeV corresponding to ≈ 10% depending upon the current. It is then obvious that the acceptance of the magnetic spectrometer is only about 10% as it is seen in Table I.

The energy spread in the linac can be explained taking into account both phase spread and beam loading in the accelerating sections. For instance a bunch with the charge of 30 nC will induce about 3.7% of energy dispersion in the SW buncher and about 13% spread in TW sections. On the other hand a bunch length of 25° for the optimum central position of the bunch with respect to the maximum of the accelerating field, will give about 3% of energy spread. An energy spread of 10 MeV (≈ 3%) is then comparable with a phase spread of 30° for a bunch on the crest of the wave. At low currents ~ 1 A from the gun corresponding to ≈ 0.1. A at the linac end) beam loading is negligible and the energy spread is nearly totally due to the phase spread. In our case the energy spread was measured at the end of the linac . Taking into account that the transmission to that point is only about 10% ,it is rather difficult to find the direct connection between this measured energy spread and eg. phase relations at the exit of the buncher.

Nevertheless it is obvious that the best conditions for acceleration and transmission of either electrons or positrons are in the central part of the bunch so the shorter is the bunch the better are conditions for acceleration of the total bunch.

Taking the above considerations into account it is obvious that even in the case of low currents when the beam loading is negligible, a bunch length of the order of 20° will be the upper limit for the phase extention at the exit of the SW buncher, to have admissible energy dispersion. But as it can be seen from the calculations made for the buncher both at CGRMeV [5] and at Frascati [4] in the case of R = E1/E2 =0.5, suggested as an optimum for bunching, the phase acceptance was about 60% and the bunch length (45-50)°. Such a large phase length of a bunch will create some difficulties for proper acceleration of the total bunch in the following TW sections:

- Since the electrons at the exit of the buncher are already relativistic it will be difficult without special arrangements (eg. magnetic compression) to shorten the bunch in order to avoid large energy spread in the TW sections.
- In the case of long bunches it is difficult to maintain the current in the bunch in perfect phase accordance with the accelerating field.E.g. the beam loading will not only increase the energy spread but also will lead to changes of effective phase of accelerating fields during the pulse and as a result to the loss of the part of the beam. [1].
- Large phase extention will not only make less effective longitudinal acceleration but also increases radial defocusing forces. (see Fig. 7)

It is then clear from above that in fact one cannot accelerate effectively the total bunch which comes out of the SW buncher, so that it is necessary to take only some partt of it. To choose properly the desired part of the bunch one should know the distribution $N(\Phi)$, where N is the number of electrons and Φ is their phase at the end of the buncher. It is obvious that the narrower this distribution , the better the conditions for further proper acceleration of the bunch. The histogram of the distibution at the exit of the buncher is presented in Fig.8; it has been obtained by tracking with PARMELA code a 10 A continuous beam produced by the gun (emittance 5×10^{-5} m rad, radial dimension 2.5 mm) through the solenoids connected with the gun and along the SW buncher section.The total transmission is 62% , the distribution is almost uniform in the interesting zone, so that taking only the useful phase spread $\Delta\phi < 20°$ means cutting the charge in the bunch to rather low values. This effect holds both for electron and positron operation but is specially important for the case of positrons: we should have a large number of electrons within a phase length less than 15 deg. to create a sufficiently large number of positrons with the required energy spread of 2%. Taking into account the histogram presented in Fig. 8 , the necesity of introducing a prebuncher system between the gun and the buncher is evident.

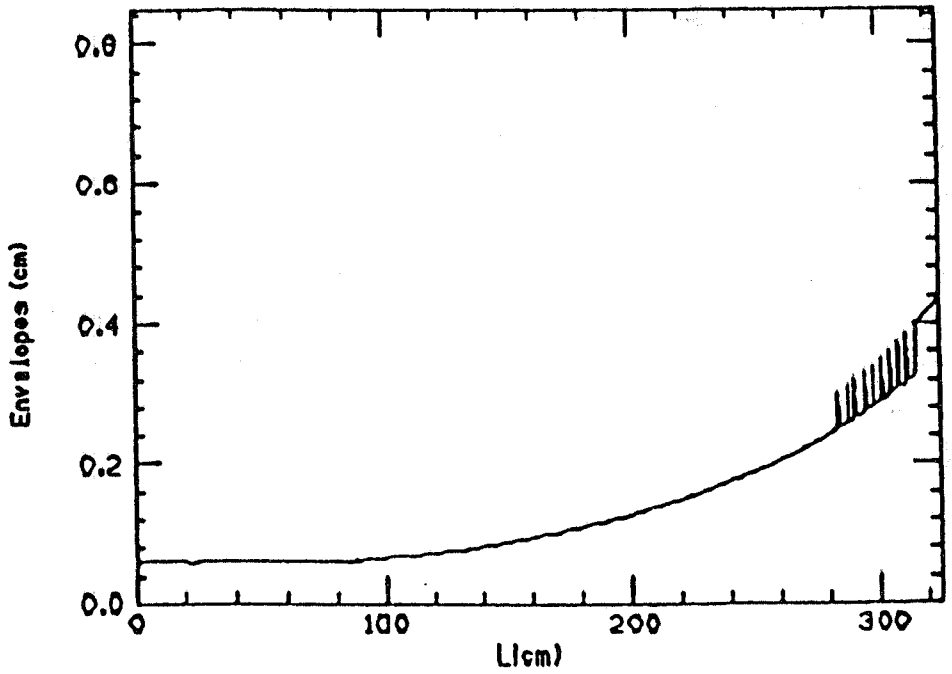

FIG. 7 - Envelope of a $\delta\phi = 30°$ bunch travelling on the rf crest.

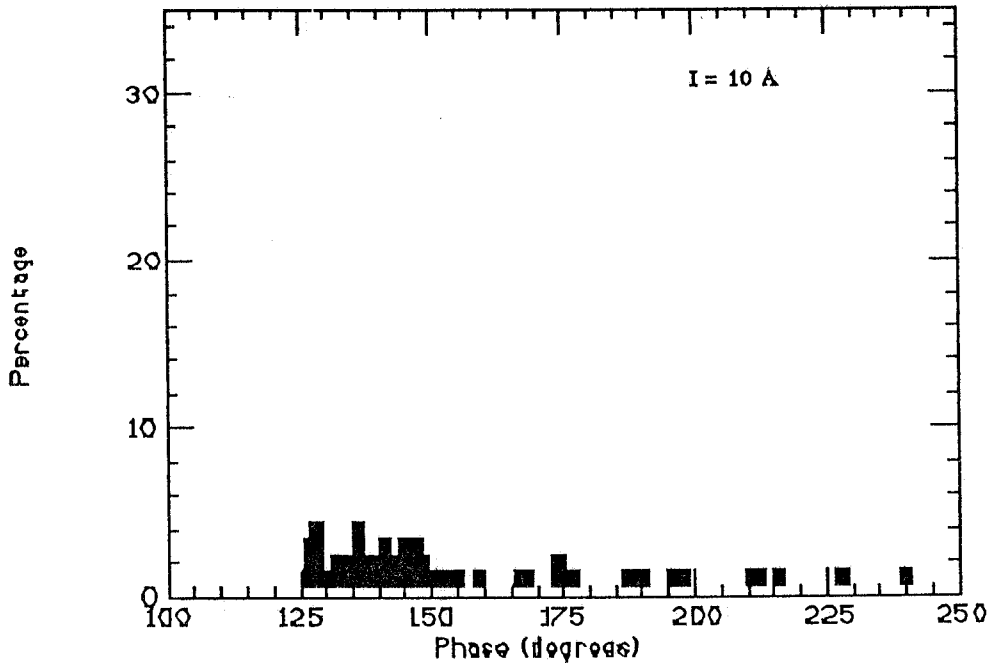

FIG. 8 - Phase distribution of the electron beam at the exit of the buncher as obtained by tracking a current of 10A from the gun in the configuration of the injection system without the prebuncher.

The prebuncher system.

The prebuncher, a single cell cavity with a field of about 10 KV over 1 cm gap, compresses ≈ 80 % of the beam into about 20 deg. after a drift space of ≈ 25 cm. The following buncher section then squeezes further this bunch.

The configuration of the prebuncher section is shown schematically in Fig. 9. It requires an extra space of ≈ 30 cm between the gun and the buncher. Due to the strong space charge force in the 100 KeV beam from the gun, it is necessary to introduce a set of solenoidal lenses to confine the beam transversely. To avoid emittance deterioration there should be no gap in the confining magnetic field.

The distribution of the magnetic field along the system results from the superposition of the fields of the pre-existing solenoids and those of the added lenses. To calculate the dynamics of the electrons in the injection system we have introduced in the code PARMELA the possibility of approximating the magnetic field configuration by the sum of gaussian profiles.

Tracking has been performed for two different situations , corresponding to the regimes of high current (I=10 A, emittance $5x10^{-5}$ m rad). The optimum magnetic field is shown in Fig. 10 for both situations, and Tab. III gives the peak values of the gaussian distributions of the magnetic fields of all the lenses, including that of the solenoid on the buncher which, lacking the information about its distribution, has been taken as uniform along the structure and with two gaussian tails at the ends. The beam envelopes are plotted in Fig. 11.

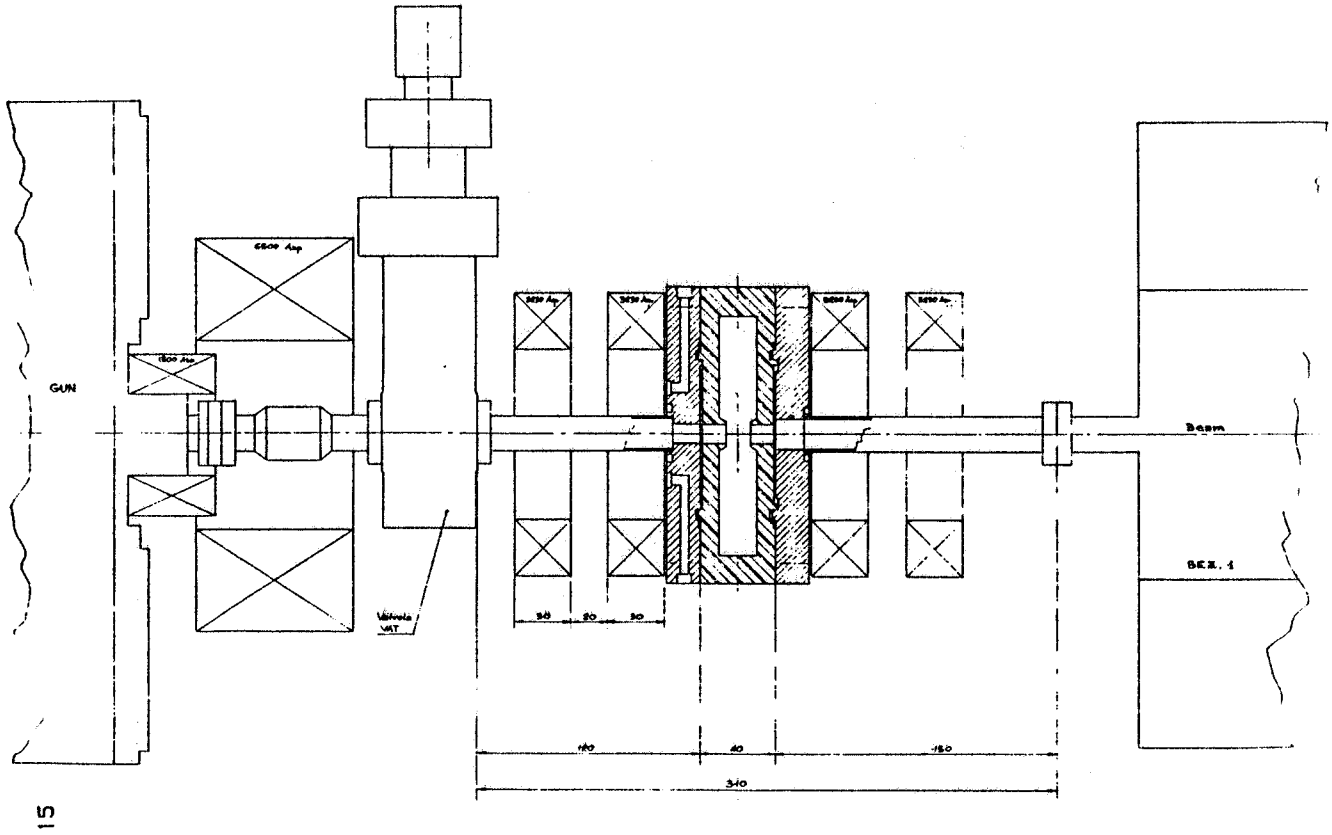

FIG. 9 - Schematic of the beginning of the linac injection system with the prebuncher.

TABLE III - The optimum magnetic field intensities of the lenses of the system.

Magnetic Field (gauss)	I_{gun} = 0.2A	I_{gun} = 10 A
B1	180.	235.
B2	370.	480.
B3	190.	240.
B4	190.	240.
B5	110.	240.
B6	110.	240.
$B_{buncher}$	1500.	1500

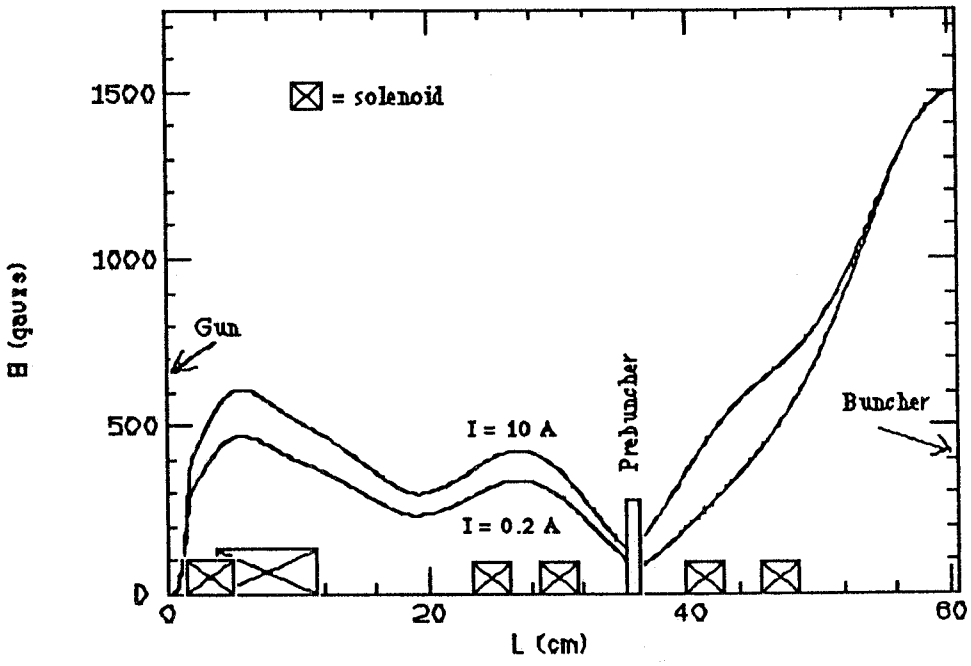

FIG. 10 - Optimum magnetic field configuration in the prebuncher system as introduced in the code PARMELA for two different currents from the gun.

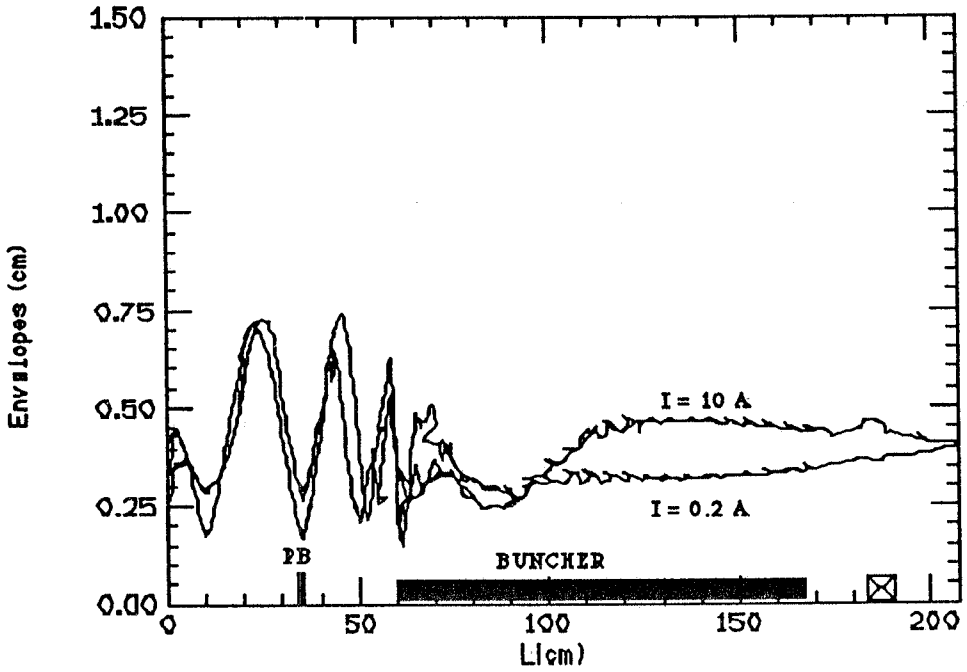

FIG. 11 - Beam envelopes along the prebuncher system, the buncher section and the solenoidal lens lastly introduced between the buncher and the subsequent linac for the two different currents.

Figs. 12 and 13 refer to the longitudinal phase space and phase distribution at the exit of the buncher . 88 % of the current is transmitted against 60% without prebuncher. From Fig. 13 it results that 60% of the current is included in a phase length of 8 deg. corresponding roughly to an order of magnitude improvement on the peak current over the preceding situation

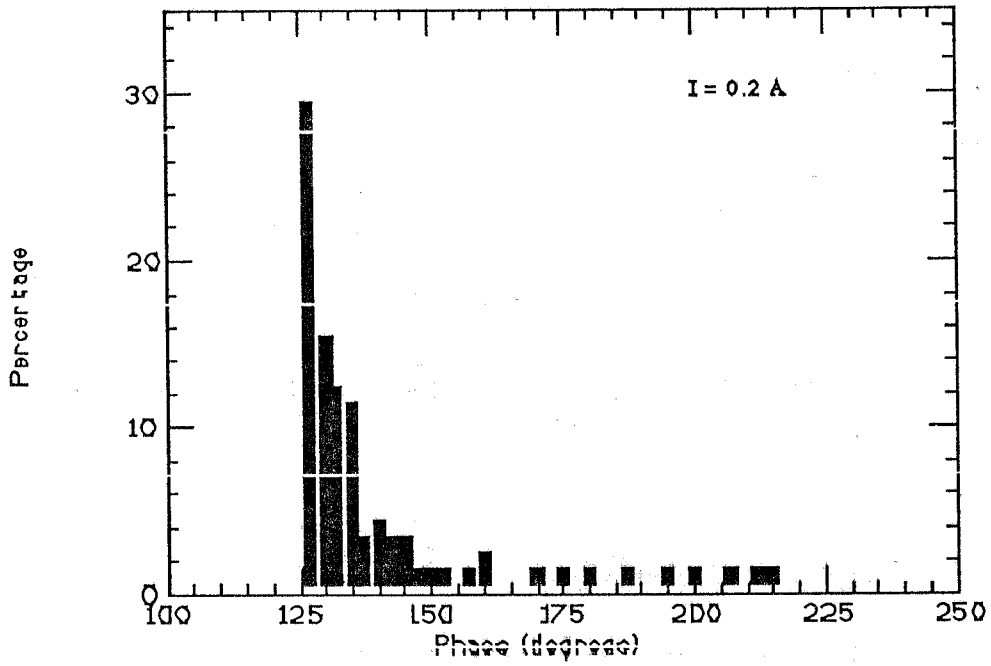

FIG. 12 - Phase distribution of the electron beam at the exit of the buncher for I_{gun} = 0.2 A with the prebuncher cavity.

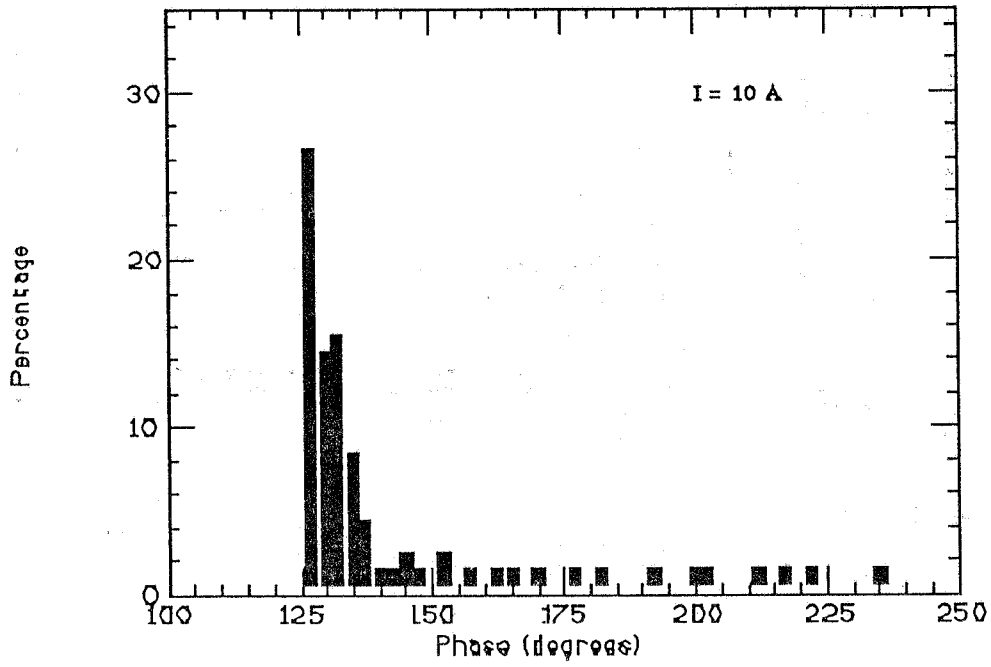

FIG. 13 - Phase distribution of the electron beam at the exit of the buncher for I_{gun} = 10 A with the prebuncher cavity.

5. - COMPARISONS OF THE RESULTS WITH AND WITHOUT PREBUNCHER

A set of measurements has been made of the functioning of the linac with and without prebuncher. The results are given in Tab. IV and also presented in Fig 14.

The main results can be summarized as follows:

- Transmission efficiency. There is practically no difference when working with and without prebuncher. It confirms the opinion that particle losses are due principally to the large beam emittance and successive beam scalloping before the buncher (I_{LE}/I_G= 0.2; I_{M2}/I_G= 0.1) and not because of small phase acceptance.
- Energy dispersion. As it results from Tab IV , the energy dispersion as measured by the magnetic spectrometer at 300 MeV is two times smaller with the prebuncher than without (8 MeV against 16 MeV). It is seen even better on Fig. 14 giving the electron current passing through the spectrometer as a function of energy. This effect already improves twice the efficiency of injection into the storage ring. In the case of positrons the improvement is still larger since with lower energy dispersion the spot of the beam on the converter can be made much smaller, increasing thus the efficiency of positron generation.

This result justifies the introduction of the prebuncher in the new injection system of ADONE.

TABLE IV - Beam transmission along the linac with prebuncher and without it.

I_g A	t_g ns	I_B A	I_{LE} A	I_{M2} A	E MeV	ΔE MeV	B_{12} A	B_{34} A	B_{56} A	B_B A
1.77	9.5	0.39	0.39	0.14	305	9	15.2	190	17	110 (*)
1.67	10	0.36	0.37	0.16	302	16	15.2	190	170	110
1.78	10	0.33	0.39	0.16		15.2	100	150	110 (*)	
1.7	10	0.32	0.39	0.17	297	8				(*)
0.6		0.15	0.09				14.2	150	150	110 (*)
5.0	9	1.1	1.0				15.2	50	50	112 (*)
6.2		1.15	0.8				15.2	50	50	112
10	9.7	3.0	3.0				15.2	180	160	110 (*)
10.6		2.9	2.5				15.2	180	160	110
14		5.5	4.7				15.2	170	175	112 (*)
14	10	3.7	4.3				15.2	170	175	112

(*)PREBUNCHER ON

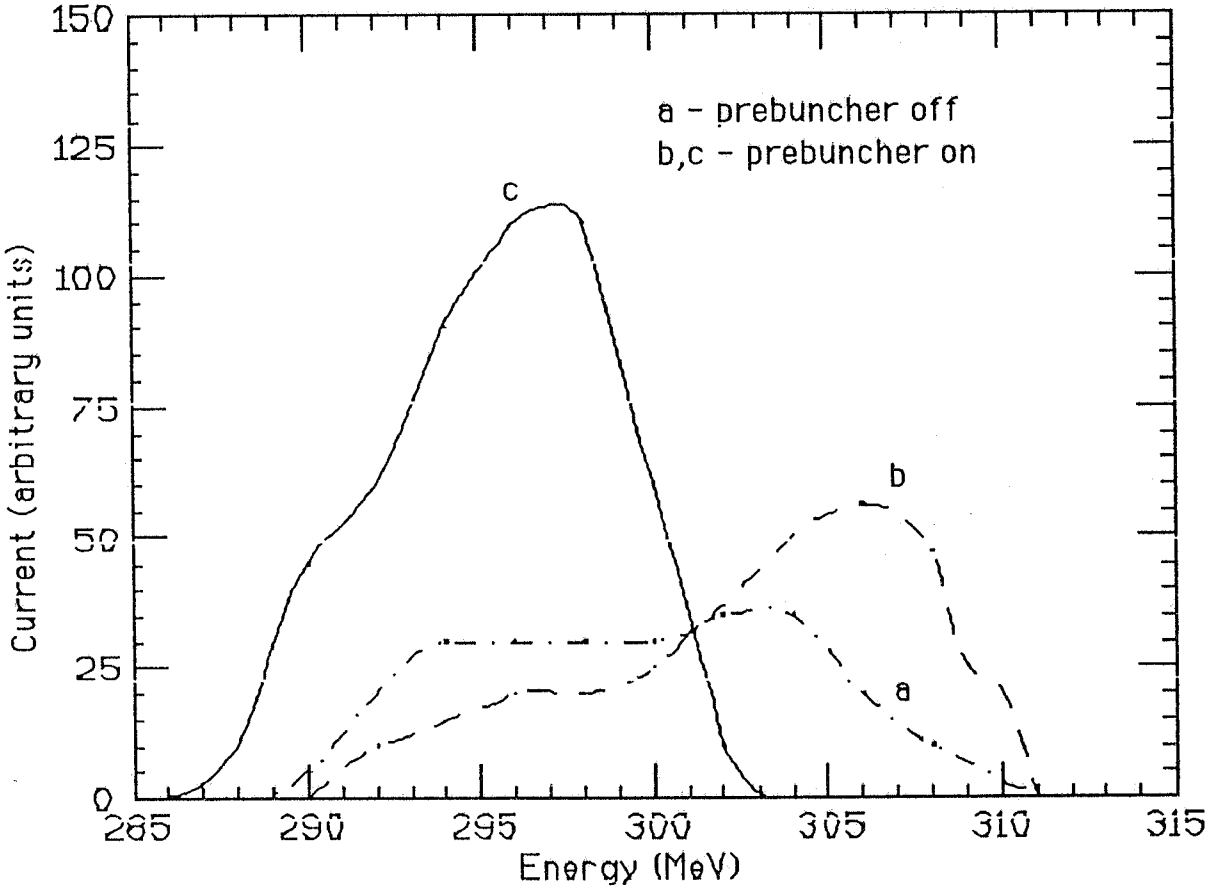

FIG. 14 - Electron energy distribution at the end of high energy linac measured by the magnetic spectrometer. Curve a - no prebuncher, curves b,c - prebuncher on.

REFERENCES

1) J. Haimson- IEEE Trans. on NS 12,499 (June 1965).
2) CGR MeV note DT 10 976 DT/NM. Dec.1985.
3) S. Kulinski , Large Signal Electron Bunching. CERN PS/LPI Note / 85-11.
4) R. Chaput, Fonctionement de la Cavite de Pre-groupement CGR - MeV a Fort Champ, LAL/PI 85 - 20/T..
5) CGR MeV note DT 11620 AS/NM Dec.1986.
6) C. Biscari , S. Kulinski, B. Spataro, F. Tazzioli, M. Vescovi - Design of a Prebuncher System for the New Standing Wave Buncher Injector of the Frascati Linac. - ADONE MEMO L - 99, Frascati July 1988.
7) M. Chiti , A. Esposito, S. Kulinski, M. Vescovi- Electron Energy Determination in the Standing Wave Buncher of ADONE by Measurements of the Thresholds of (γ,n) Induced Reactions - ADONE MEMO L- 100. Frascati September 1988.